INSTITUTE OF PHYSICS PUBLISHING SUPERCONDUCTOR SCIENCE AND TECHNOLOGY

Supercond. Sci. Technol. **18** (2005) 1275–1279 doi:10.1088/0953-2048/18/10/005

Relationship between microstructure and J_c property in MgB_2/α-Al_2O_3 film fabricated by *in situ* electron beam evaporation

H Sosiati[1,2,7], S Hata[2], N Kuwano[3], Y Tomokiyo[2], H Kitaguchi[4], T Doi[5], H Yamamoto[6], A Matsumoto[4], K Saitoh[6] and H Kumakura[4]

[1] HVEM, Kyushu University, Fukuoka 812-8581, Japan
[2] ASEM, Kyushu University, Kasuga 816-8580, Japan
[3] ASTEC, Kyushu University, Kasuga 816-8580, Japan
[4] National Institute for Materials Science, Tsukuba 305-0047, Japan
[5] Faculty of Engineering, Kagoshima University, Kagoshima 890-0065, Japan
[6] Advanced Research Laboratory, Hitachi Ltd, Kokubunji 185-8601, Japan

E-mail: harini@astec.kyushu-u.ac.jp

Received 18 May 2005, in final form 6 July 2005
Published 9 August 2005
Online at stacks.iop.org/SUST/18/1275

Abstract

A transmission electron microscopy (TEM) study has been carried out on an MgB_2/α-Al_2O_3 film that exhibits the typical property of critical current density (J_c) under magnetic fields. The MgB_2 layer of 300 nm in thickness was grown on a (001)α-Al_2O_3 substrate using an *in situ* electron beam evaporation method. J_c of the film takes significantly high values when the applied magnetic field is perpendicular to the film surface. The MgB_2 layer consists of fine columnar MgB_2 crystals 20–30 nm in size. The columnar MgB_2 crystals grow almost perpendicular to the substrate surface and have no crystallographic orientation relationship with the α-Al_2O_3 substrate because of an amorphous layer formed first on the substrate. A high density of columnar grain boundaries within the MgB_2 layer may be effective for the enhancement of the flux-pinning under the perpendicular magnetic field.

1. Introduction

Soon after the discovery of MgB_2 with high critical temperature ($T_c \sim 39$ K) and critical current density (J_c) under high magnetic fields [1], research work on the MgB_2 as a promising superconducting material has strongly increased. In order to extend large-scale applications of the MgB_2 superconductor to electronic devices, many efforts have been carried out to grow MgB_2 thin films on sapphire (α-Al_2O_3) single-crystal substrates using various fabrication techniques such as carrousel sputtering [2], electron beam evaporation (EBE) [3], hybrid physical–chemical vapour deposition (HPCVD) [4] and pulsed-laser deposition (PLD) techniques [5]. Experimental parameters such as annealing conditions, the substrate temperature and the cut-plane of substrates have been found to influence microstructures and electrical properties of MgB_2 films [2, 6, 7].

Here we focus on a pronounced influence of microstructure in MgB_2 films on their J_c properties under magnetic fields reported by Kitaguchi *et al* [3]. They fabricated $MgB_2/(001)\alpha$-Al_2O_3 thin films by the *in situ* EBE method. The fabricated films show a fine columnar grain structure of MgB_2 20–30 nm in size and exhibit significantly high J_c values when the applied magnetic field is perpendicular to the film surface. They suggested that grain boundaries between the fine columnar MgB_2 crystals work as strong flux-pinning sites under the perpendicular magnetic fields. This J_c property is different from those of other MgB_2/α-Al_2O_3 films fabricated by the *in situ* HPCVD and the two-step PLD methods [4, 5],

[7] Corresponding address: Art, Science and Technology Center for Cooperative Research, Kyushu University, 6-1 Kasuga Kouen, Kasuga-shi, Fukuoka 816-8580, Japan.

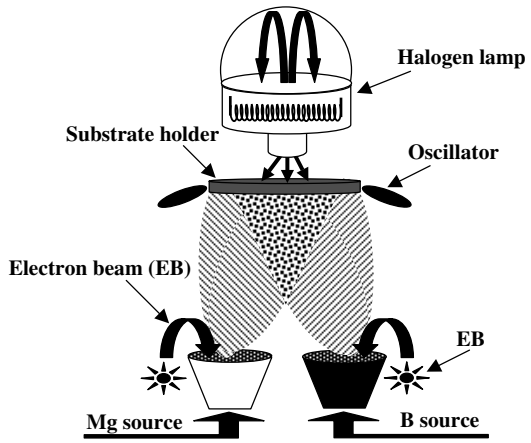

Figure 1. Schematic illustration of an electron beam evaporation technique.

since these MgB_2 films show higher J_c values under parallel magnetic fields than perpendicular fields to the film surface. Kitaguchi *et al* [3] explained that the difference in the J_c property is due to microstructural differences. However, no detailed investigation of the microstructure in the EBE films has been reported.

In this study, we investigated the microstructure in the EBE MgB_2 film by TEM. J_c of this EBE film was measured under various directions of the magnetic field. Influences of the microstructure on the J_c property under magnetic fields will be discussed.

2. Experimental details

The MgB_2 layer of about 300 nm in thickness was grown on a (001)α-Al_2O_3 substrate using the *in situ* EBE technique, as schematically illustrated in figure 1. The substrate was heated at 543($\pm$5) K with a lamp heating system during the EBE process. The base pressure was controlled to less than 10^{-6} Pa. As evaporation sources, a magnesium ingot and boron crystals with particle sizes of 5–10 nm were evaporated at the same time. The evaporation flux ratio of magnesium and boron was set to 4:1, and the growth rate of the MgB_2 film was 1 nm s^{-1}.

The critical current I_c was measured by the four-probe method. Ag wires and In solder were used for current and voltage contacts and 1 μV cm^{-1} criterion was employed for I_c determination. The I_c measurement was made at 4.2 K under various directions of the magnetic field. J_c was calculated by dividing the I_c value by the cross-sectional area of the film.

Cross-sectional TEM specimens of the MgB_2 thin film were prepared with a focused ion beam (FIB) microsampling technique. TEM observations were carried out with an FEI TECNAI-F20 electron microscope that is equipped with scanning TEM (STEM) and energy dispersive x-ray spectroscopy (EDS) systems. In addition to conventional and high-resolution TEM observations, two-dimensional STEM-EDS elemental mapping was performed. The electron probe size for the STEM-EDS analysis was about 1 nm.

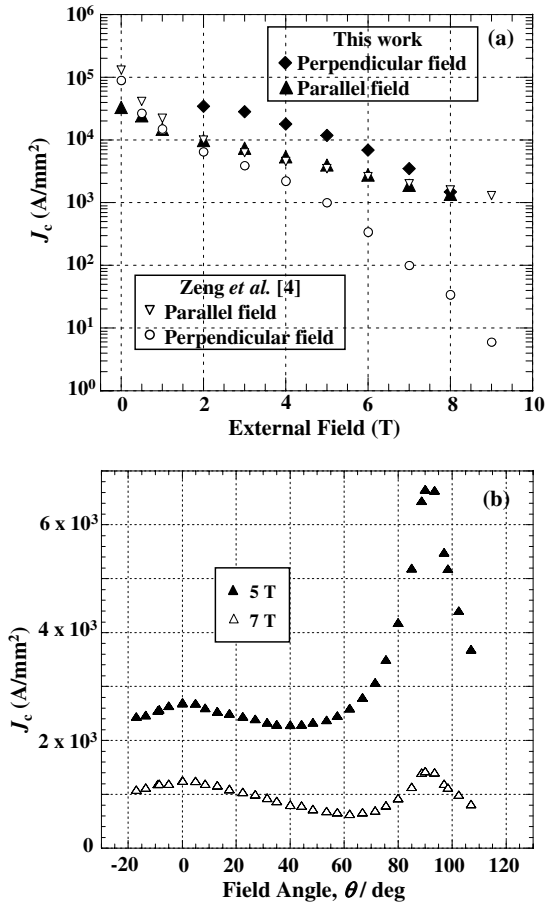

Figure 2. (a) J_c as a function of magnetic field and (b) J_c as a function of θ, angle between the direction of the magnetic field and the film surface.

3. Results and discussion

3.1. J_c property

Figure 2(a) shows J_c values of the present EBE film under magnetic fields parallel ($\theta = 0°$) or perpendicular ($\theta = 90°$) to the film surface. θ is the angle between the direction of the magnetic field and the film surface. In this study, we define that $\theta = 0°$ and $\theta = 90°$ are parallel field and perpendicular field, respectively. At the same magnitude of magnetic fields up to 7 T, J_c for $\theta = 90°$ is higher than that for $\theta = 0°$. This trend of J_c between $\theta = 0°$ and 90° is reversed under magnetic fields over 8 T. A more detailed dependence of J_c on θ is depicted in figure 2(b). J_c around $\theta = 90°$ is significantly higher than that around $\theta = 0°$, which suggests a strong flux pinning when the applied magnetic field is perpendicular to the film surface, as described above [3]. Figure 2(a) also shows J_c values of an MgB_2/(001)α-Al_2O_3 thin film fabricated by the HPCVD method (after Zeng *et al*) [4]. From a comparison of J_c between the EBE and HPCVD films, it can again be confirmed that the EBE MgB_2 film in the present work exhibits very high J_c under the perpendicular magnetic fields.

3.2. TEM and STEM-EDS analyses

Figures 3(a) and (b) display bright field images in different areas of the EBE MgB_2 film with the incident beam along

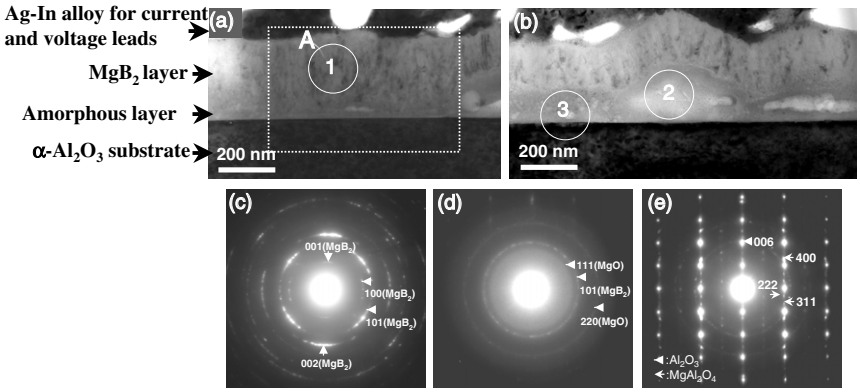

Figure 3. (a), (b) Cross-sectional bright field images in different areas of an $MgB_2/(001)\alpha$-Al_2O_3 film. (c)–(e) Electron diffraction patterns obtained from encircled areas '1', '2' and '3' in the bright field images in (a) and (b), respectively.

the $[\bar{1}\bar{2}0]$ zone axis of the α-Al_2O_3 substrate. An electron diffraction pattern in figure 3(c) taken from encircled area '1' in the bright field image (a) exhibits ring patterns of the MgB_2 phase. This suggests that the *in situ* EBE method produced a crystalline MgB_2 layer about 200–300 nm in thickness containing no other phases such as MgO, $Mg(B, O)_2$ [8] and MgB_4. Such impurity phases are often formed in MgB_2 films fabricated with the PLD technique [9–12]. An intermediate layer of 50–200 nm in thickness is formed between the MgB_2 layer and the α-Al_2O_3 substrate. A diffraction pattern in figure 3(d) taken from encircled area '2' in (b) suggests that the intermediate layer contains MgB_2 and MgO. Figure 3(d) also exhibits halo intensity that indicates the existence of amorphous phases in the intermediate layer. A diffraction pattern in figure 3(e) taken from encircled area '3' in (b) indicates the formation of an $MgAl_2O_4$ phase at the interface between the intermediate layer and the α-Al_2O_3 substrate. Such a formation of the $MgAl_2O_4$ phase on the α-Al_2O_3 substrate has been reported previously [13, 14].

An HRTEM image in figure 4 reveals detailed microstructures of the region around the intermediate layer, the $MgAl_2O_4$ layer and the α-Al_2O_3 substrate. In the intermediate layer, lattice fringes corresponding to nano-crystalline MgB_2 or MgO, as marked by arrows, are recognized, but small in number. This suggests that amorphous phases are predominantly present in the intermediate layer. Thus, we regard this layer as 'an amorphous layer'. The $MgAl_2O_4$ layer of 20–30 nm in thickness is epitaxially formed on the α-Al_2O_3 substrate and the $MgAl_2O_4/\alpha$-Al_2O_3 interface is not flat at the atomic scale.

The formation of the amorphous layer and $MgAl_2O_4$ layer can be interpreted as follows. In the early stage of the *in situ* EBE process using the lamp heating system, the substrate would not immediately heat up to the desired temperature (543 K) since the α-Al_2O_3 substrate is transparent. Furthermore, the growth rate, 1 nm s^{-1}, is much higher than typical ones, for example, about 0.04 nm s^{-1} in [6]. This growth condition is considered to lower the crystallinity of MgB_2. It is thus possible that amorphous phases were formed together in the early stage of nucleation and growth of MgB_2 crystals. The thickness of the amorphous layer is not uniform. This may be due to inhomogeneous heat distribution on the substrate surface. More detailed reasons are

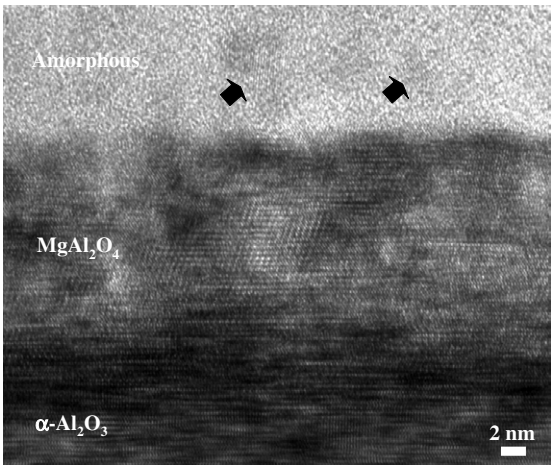

Figure 4. A high-resolution image of the interface region between the amorphous layer and the α-Al_2O_3 substrate. Arrows indicate lattice fringes corresponding to nanocrystalline MgB_2 or MgO.

now being investigated. Due to the different evaporation rates of magnesium and boron, 2 and 0.5 nm s^{-1}, respectively, the magnesium atoms would firstly accumulate on the substrate surface. It is possible that there was residual oxygen contaminant on the substrate surface. Hence, such excess magnesium atoms would be oxidized to MgO and then diffuse into the α-Al_2O_3 substrate to form the $MgAl_2O_4$ phase. Due to very high reactivity of Mg to oxygen, some of the unreacted Mg atoms in the intermediate layer would be oxidized in the air after the film fabrication.

Figure 5 shows magnified images of area 'A' marked in figure 3. The dark field image in figure 5(c) taken with the 002(MgB_2) reflection clearly shows fine granular grains of 5 nm or less in size near the substrate surface. These granular MgB_2 crystals were formed in the early stage of the EBE process at low substrate temperatures. Columnar MgB_2 crystals grown above the granular ones contain high density of grain boundaries along the columnar growth direction. It is explained that the granular MgB_2 crystals near the substrate grew into columnar ones as the substrate temperature rose.

Figure 6 displays an STEM-EDS elemental mapping result. From the oxygen map in (b), no oxygen distribution

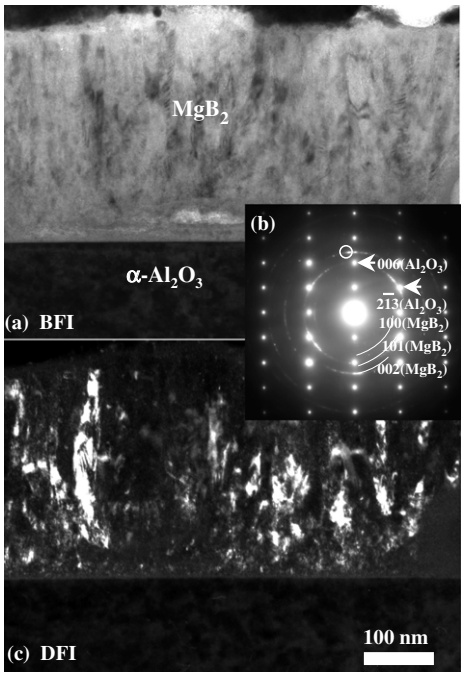

Figure 5. A higher magnification image of area 'A' marked in figure 3. (a) A bright field image, (b) an electron diffraction pattern taken from the interface region of the MgB_2 layer/α-Al_2O_3 substrate and (c) a dark field image taken with a part of the diffraction ring marked with a small circle in (b).

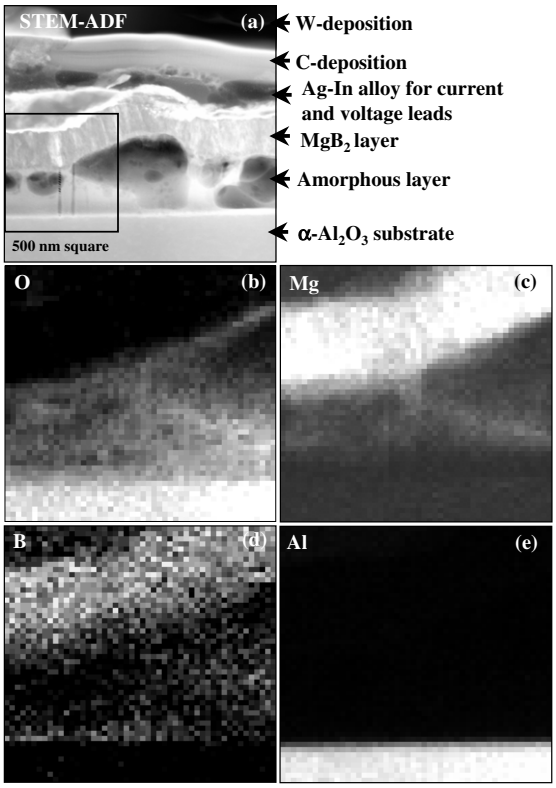

Figure 6. STEM-EDS elemental mapping of an MgB_2/(100)α-Al_2O_3 film. (a) A bright field STEM image, (b) O-K map, (c) Mg-K map, (d) B-K map and (e) Al-K map.

appears in the MgB_2 layer. This confirms that the MgB_2 layer is free from oxide phases. The amorphous layer contains oxygen (b), magnesium (c) and boron (d). Therefore, in addition to the nano-crystalline MgO, some oxide phases such as BO_x [15, 16] and $Mg(B, O)_2$ [8] may exist in the amorphous layer. The Al map in (e) confirms that Al atoms in the Al_2O_3 substrate do not diffuse into the MgB_2 layer.

3.3. Relationship between microstructure and J_c behaviour under magnetic fields

As described above, Zeng *et al* [4] have reported the dependence of J_c on θ in the MgB_2 film fabricated by the *in situ* HPCVD method. This MgB_2 film does not exhibit the enhancement of J_c under fields perpendicular to the film surface, as shown in figure 2(a). From cross-sectional TEM observations, the HPCVD MgB_2 film of about 300 nm in thickness has a columnar grain structure with grain sizes larger than 100 nm. The columnar MgB_2 crystals are epitaxially grown on the substrate. Plan-view observations of the columnar grain structure revealed that the MgB_2 crystals have hexagonal shapes and exhibit the same crystallographic orientation relationship with the substrate. These facts suggest that grain boundaries between the columnar MgB_2 crystals have similar characters to each other from the viewpoint of atomic structure. On the other hand, the EBE MgB_2 film in the present work shows finer columnar MgB_2 crystals (20–30 nm), resulting in much higher density of grain boundaries along the columnar growth direction. The fine columnar MgB_2 crystals are rather irregular in shape (figure 5) and have no crystallographic orientation relationship with the substrate because of the existence of the amorphous layer. Therefore, it is expected that various kinds of grain boundary structure exist within the EBE film. This typical columnar grain structure is attributed to the significant enhancement of flux-pinning under magnetic fields perpendicular to the substrate surface.

4. Conclusions

TEM study on the MgB_2/α-Al_2O_3 thin film fabricated by *in situ* electron beam evaporation has been carried out. The following conclusions were obtained.

(1) The MgB_2 layer is characterized by fine columnar grains of 20–30 nm in size growing almost perpendicular to the substrate surface. No impurity phase is observed within the MgB_2 layer.

(2) The amorphous and $MgAl_2O_4$ layers are formed between the MgB_2 layer and the α-Al_2O_3 substrate. The amorphous layer contains nanocrystalline MgB_2 and MgO.

(3) High density of columnar grain boundaries within the MgB_2 layer may work as effective pinning sites. The pinning force of the columnar grain boundaries is stronger than that of the interface between the MgB_2 layer and the amorphous layer, resulting in higher J_c under perpendicular magnetic fields than that under parallel fields.

Acknowledgments

This work was supported in part by Nanotechnology Support Project of the Ministry of Education, Culture, Sports, Science and Technology (MEXT), Japan and Research Promotion Bureau, MEXT, Japan under the contracts No. 16-556.

References

[1] Nagamatsu J, Nakagawa N, Muranaka T, Zenitani Y and Akimitsu J 2001 *Nature* **410** 63–4
[2] Saito A, Kawakami A, Shimakage H and Wang Z 2002 *Supercond. Sci. Technol.* **15** 1325–9
[3] Kitaguchi H, Matsumoto A, Kumakura H, Doi T, Yamamoto H, Saitoh K, Sosiati H and Hata S 2004 *Appl. Phys. Lett.* **85** 2842–4
[4] Zeng X H *et al* 2002 *Nat. Mater.* **1** 1–4
[5] Choi E M, Gupta S K, Sen S, Lee H S, Kim H J and Lee S I 2004 *Supercond. Sci. Technol.* **17** S524–7
[6] Mori Z, Doi T, Eitoku K, Ishizaki Y, Kitaguchi H, Okada M, Saitoh K and Hakuraku Y 2004 *Supercond. Sci. Technol.* **17** 47–50
[7] Moon W-J, Kaneko K, Toh S, Saunders M, Saito A, Wang Z, Abe H and Naito M 2004 *Supercond. Sci. Technol.* **18** 92–100
[8] Liao X Z, Serquis A, Zhu Y T, Huang J Y, Civale L, Peterson D E, Mueler F M and Xu H F 2003 *J. Appl. Phys.* **93** 6208–14
[9] Bugoslavsky Y *et al* 2002 *Supercond. Sci. Technol.* **15** 1392–7
[10] Sosiati H, Hata S, Kuwano N, Tomokiyo Y, Matsumoto A, Fukutomi M, Kitaguchi H, Komori K and Kumakura H 2004 *Physica* C **412–414** 1376–82
[11] Hata S, Sosiati H, Tomokiyo Y, Kuwano N, Matsumoto A, Fukutomi M, Kitaguchi H, Komori K and Kumakura H 2004 *J. Japan. Inst. Met.* **68** 648–55
[12] Hata S, Sosiati H, Kuwano N, Tomokiyo Y, Matsumoto A, Fukutomi M, Kitaguchi H, Komori K and Kumakura H 2005 *IEEE Trans. Appl. Supercond.* **15** 3238–41
[13] Tian W, Pan X Q, Bu S D, Kim D M, Choi J H, Patnaik S and Eom C Bb 2002 *Appl. Phys. Lett.* **81** 685–7
[14] Bu S D *et al* 2002 *Appl. Phys. Lett.* **81** 1851–3
[15] Klie R F, Idrobo J C, Browning N D, Regan K A, Rogado N S and Cava R J 2001 *Appl. Phys. Lett.* **79** 1837–9
[16] Dou S X, Braccini V, Soltanian S, Klie R, Zhu Y, Li S, Wang X L and Larbalestier D 2004 *Supercond. Sci. Technol.* **96** 7549–55